Pak. J. Bot., 49(5): 1627-1640, 2017.

IDENTIFICATION OF CANDIDATE PROTEINS AND NETWORKS RELATED TO SALINITY STRESS IN SHRUB WILLOW ROOTS BY COMPARATIVE PROTEOMIC ANALYSIS

SUI DEZONG[1,2*],WANG BAOSONG[2], XU LIAN[1] AND SHI SHIZ ENG[2]

[1]Co-Innovation Center for Sustainable Forestry in Southern China, Nanjing Forestry University, Nanjing 210037, Jiangsu, China, [2]Jiangsu Academy of Forestry, Nanjing 211153, Jiangsu, China
[*]Corresponding author's email: 535122107@qq.com

Abstract

Salinity stress is one of the major abiotic stresses that limit plant growth. To understand the mechanism of shrub willow clones roots in response to salt stress and explore candidate proteins for plant breeding associated with salt stress, the total proteins from seedling roots of salt-sensitive cultivar JW9-6 and salt-tolerant cultivar JW2372 under salt stress for 2, 12 and 72 h, respectively, were analyzed by 2-D electrophoresis. Finally, 109 differentially expressed proteins were successfully identified by MALDI-TOF/TOF MS. By analyzing and camparing functions of the differentially expressed proteins, obtaining the conclusions as follows: 1) the majority functions including BP (metabolic process and protein folding), CC (cytoplasm and cell) and MF (cofactor, coenzyme binding and isomerase activity), regulated by root proteins, were differences between JW9-6 (salt-sensitive) and JW2372 (salt-tolerance) under salt stress; 2) six pathways were changed by salt stress, including pyruvate metabolism, glycolysis, ascorbate and aldarate metabolism, amino sugar and nucleotide sugar metabolism, pentose phosphate pathway, and cysteine and methionine metabolism; 3) the five proteins including glucose-6-phosphate isomerase, ATP synthase epsilon chain, phosphoglycerate kinase, S-adenosylmethionine synthase 4 and adenosine kinase, could be candidate proteins for plant breeding associated with salt stress; 4) differences from the salt-responsive pathways between leaves and roots in the shrub willow clones could provide an important strategy for forest tree breeding involved in salt tolerance.

Key words: Shrub willow roots, Salt stress, Proteomic, 2-D electrophoresis, MALDI-TOF/TOF MS.

Introduction

Salt is an important factor of abiotic stress that limit plant growth and development (Ma *et al.,* 2014). About 20-50% from the whole arable land is affected by salinity stress every year (Xu *et al.,* 2011). Salinization of arable land is seriously and expected to 30% by the year 2030, and up to 50% with in the next 30 years (Wang *et al.,* 2003; Espartero *et al.,* 1994). These alkaline and saline land lead to the ecological environment destroyed and forest rarity. Shrub willow (*Salix* spp.) has characteristics such as grows apace, wide adaptation andmost extensive tree species distributed in the world. The number of willow species was at least 200 species and most of them were salt-tolerance to some extent, including *salix mongolica, Salix triandra, S. integra Thrnb,* and *JW* 2372 (Sui *et al.,* 2011). So, screening new genotypes of salt tolerance has become an important programs for forestry breedling. Discovering the new strategies and exploring molecular mechanism conferring salt stress to shrub willow will be useful for breeding of salt-tolerant forestry.

Two genotypes, JW2372 (salt-tolerance) and JW9-6 (salt-sensitive), have been used widely to open out forestry responses to salinity stress at molecular and physiological levels by many scientific personnel (Sui *et al.,* 2015). In our previous study, 83 differentially expressed proteins were found in shrub willow leaves after salt stress by 2-DE and grouped into 11 groups. The results from previous research as follows: 1) increased ROS scavenging capacity result in enhancing salt tolerance for shrub willow; 2) different means, e.g., protein folding and assembly, the depressing of protein synthesis, and increasing protein proteolysis, were important factors for shrub willow leaves responding to salinity; 3) salinity could change the pathways of carbohydrate metabolism, photosynthesis, amino acid and nitrogen metabolism, and energy supply (Sui *et al.,* 2015). However, due to the direct effects of soil salt stress on plant roots, plant roots are found to be more sensitive than leaves to salt stress (Bernstein & Meiri, 2004; Luo *et al.,* 2005). Many processes have been reported to become dominant at the proteome level in root salt response (Zhao *et al.,* 2013). Therefore, the differentially expressed proteins identified in shrub willow roots under salt stress could be essential for helping us in understanding mechnisms of shrub willow responses to salinity.

In the our research, shrub willow materials as previous study, two-dimensional gel electrophoresis (2-DE) technology was used to seedling roots of two shrub willow clones genotypes, JW2372 (salt-tolerant) and JW9-6 (salt-sensitive) for: 1)investigating the expression pattern of proteome in shrub willow roots; 2) identifing the differentially expressed proteins from shrub willow roots response to salinity; 3) understanding the pathways involved in different expressed proteins in the shrub willow clones seedling roots; 4) combined with our previous study, revealing the differences in metabolic pathways between the leaves and roots from the two shrub willow genotypes; 5) exploring candidate proteins for plant breeding associated with salt stress. Best results will help us understand clearly the possible mechanism occurring in salt-treated shrub willow seedlings.

Materials and Methods

Plant materials: Two Shrub willow clones (salt-tolerant variety JW2372 and salt-sensitive variety JW9-6) were planted in 1/4 Hoagland nutrient solution, which was replaced with fresh one every seven days. For the analogy of salinity stress, the method was conducted according to

Sui *et al*., with some modifications (Sui *et al.,* 2015). The seedlings were grown in a growth chamber with 22-28°C temperature in greenhouse of research institute of Jiangsu academy of forestry. Six-week-old seedlings were planted in each ampulla (300 ml) with 1/4 Hoagland nutrient solution including 3% NaCl, and the control were planted in 1/4 Hoagland nutrient solution. Root samples which was taken at different salinity stress time points (0, 2, 12 and 72 h) were immediately frozen in liquid nitrogen or stored at −70°C. The roots from the unstressed Shrub willow clones were also sheared at 2, 12 and 72 h, respectively, and used as control.

Protein extraction: To minimize errors, three biological samples were conducted for proteome analysis at each treated time point. Willow roots were extracted with the method of acetone/TCA precipitation according to Parker *et al*., with some modifications (Parker *et al.,* 2006). Briefly, the powder of root samples was suspended in 10% w/v trichloroacetic acid/acetone with 1% (w/v) DTT and held at -20^{o}C for 2h. After centrifugation (15000 rpm, 15 min) and rinse, the protein concentration of the root was measured at 595nm by the method of Bradford (Bradford, 1976), using bovine serum albumin as the standard.

Separation and analysis of differentially expression proteins: The separation method of total proteins used 2-D electrophoresis. The first-dimensional electrophoresis was performed on an IPG-phor IEF system (Bio-Rad, Hercules, CA, USA) (Ma *et al.,* 2012). About 1000μg protein was added in two-dimensional rehydration buffer (4% w/v CHAPS, 0.5% v/v IPG buffer, 2 M thiourea, and 7M urea) and added to each commercially available IPG strip (24-cm non-linear, pH 4–7), and then rehydrated at 50V for 13h at 20°C. Then procedure of IEF was performed under the following parameters: 200V for 1h, 500V for 1h, 1000V for 2h, 8000V for 4h, and 8000V achieving 110,000VH. Before the second-dimensional electrophoresis, the IPG strips were equilibrated for 15 min in 10 ml of reducing equilibration buffer [6 M urea, 0.375 M Tris–HCl (pH 8.8), 2% (w/V) SDS, 20% glycerol (V/V), and 2% (w/V) DTT] and then placed for another 15 min in alkylating equilibration buffer containing 2.5 % (w/V) iodoacetamide instead of 2 % DTT.

The second electrophoretic dimension was by 12% SDS-PAGE. Gel electrophoresis was carried out at 16^{o}C with a 1.0 W/gel for 1 h and then with 10 W/gel until the dye front reached about 1 cm from the bottom of the gel. The signal was visualised by silver. Gel image was digitalized with a Bio-Rad FluorS system and analyzed with PDQuest software (Version 7.1.0; BioRad). Spots of protein were detected and matched automatically on the basis of total density of gels. For each spot, the mean relative volume was assumed to its expression level at every stage. The spots showing a mean RV that changed more than 1.5 fold or less than 0.66 fold ($p<0.05$) were considered to be differentially expressed protein spots.

In-gel digestion and identification of proteins: Differentially expression proteins on gels were manually excised from gels, washed with double-distilled water, destained twice with 30 mM $K_3Fe(CN)_6$ for silver staining spots, reduced with 10 mM DTT in 50 mM NH_4HCO_3 and alkylated with 40 mM iodoacetamide in 50 mM NH_4HCO_3. The gel were dried with 100% acetonitrile and digested overnight at 37^{o}C with sequencing grade modified trypsin (Promega, Madison, WI, USA) in 50 mM NH_4HCO_3. The result peptides were extracted twice with 0.1% TFA in 50% acetonitrile (Tang *et al.,* 2008). The samples were air-dried and analyzed with a 4800 MALDI-TOF/TOF Proteomics Analyzer (Applied Biosystems, USA).

All raw datas of proteins were searched on the internet using a Mascot search engine, against Uniprot databases. The searching parameters were setted as follows: taxonomic category restrictions to *Populus trichocarpa*. 120 ppm mass tolerance for peptides and 0.5 Da mass tolerance of TOF/TOF fragments, cysteines carbamidomethylation as a fixed modification and methionine oxidation as a variable modification. The confidence in the peptide mass fingerprinting matches ($p<0.05$) was based on the MOWSE score and confirmed by the accurate overlapping of the matched peptides with the major peaks of the mass spectrum. Only significant hits, as defined by the MASCOT probability analysis ($p<0.05$), were accepted.

Analysis of GO and KEGG pathway enrichment: The DAVID toolkit (http://david.abcc.ncifcrf.gov), was used to analyze the obtained proteomics data, in which distributions in biological processes, cell components and molecular functions were assigned to each protein based on Gene Ontology (GO) database. For Kyoto Encyclopedia of Genes and Genomes (KEGG) pathway enrichment was performed using annotated proteins in the query dataset against the KEGG database. Protein-protein interaction (PPI) analysis was using String and Cytoscape software (Sun *et al.,* 2015), in which confidence cutoff of 400 was used: Interactions with bigger confident score were show as solid lines between genes/proteins, otherwise in dashed lines.

Results

Separation and identification of differentially expressed proteins: To investigatethe changes of total proteins (0, 2, 12, and 72 h) between the two genotypes after salinity stress, 2-D electrophoresis experiments were carried out using IEF on 24 cm pH4–7 nonlinear IPG gels. And the results indicated that more than 900 proteins could be reproducibly detected mainly in the scope of pH 4-7 (Fig. 1). Analysis of quantitative image from three biological replicates of each sample by PDQuest software revealed that a total of 124 spots showed a more than 1.5-fold or less than 0.66-fold difference ($p<0.05$) in expression values in at least one salt stress time point compared to the control. The 124 protein spots from 2-D electrophoresis gels were excised and in-gel digested using trypsin and subjected to MALDI-TOT-TOF mass spectrometry analysis. Ultimately, 109 proteins, shown in Fig. 1, were reliably identified on the basis of *Populus trichocarpa* protein database from Uniprot database (Table 1). Among which 91 were observed to be differentially expressed in genotypes JW9-6 (salt-sensitive) and 78 in cultivars JW2372 (salt-tolerance).

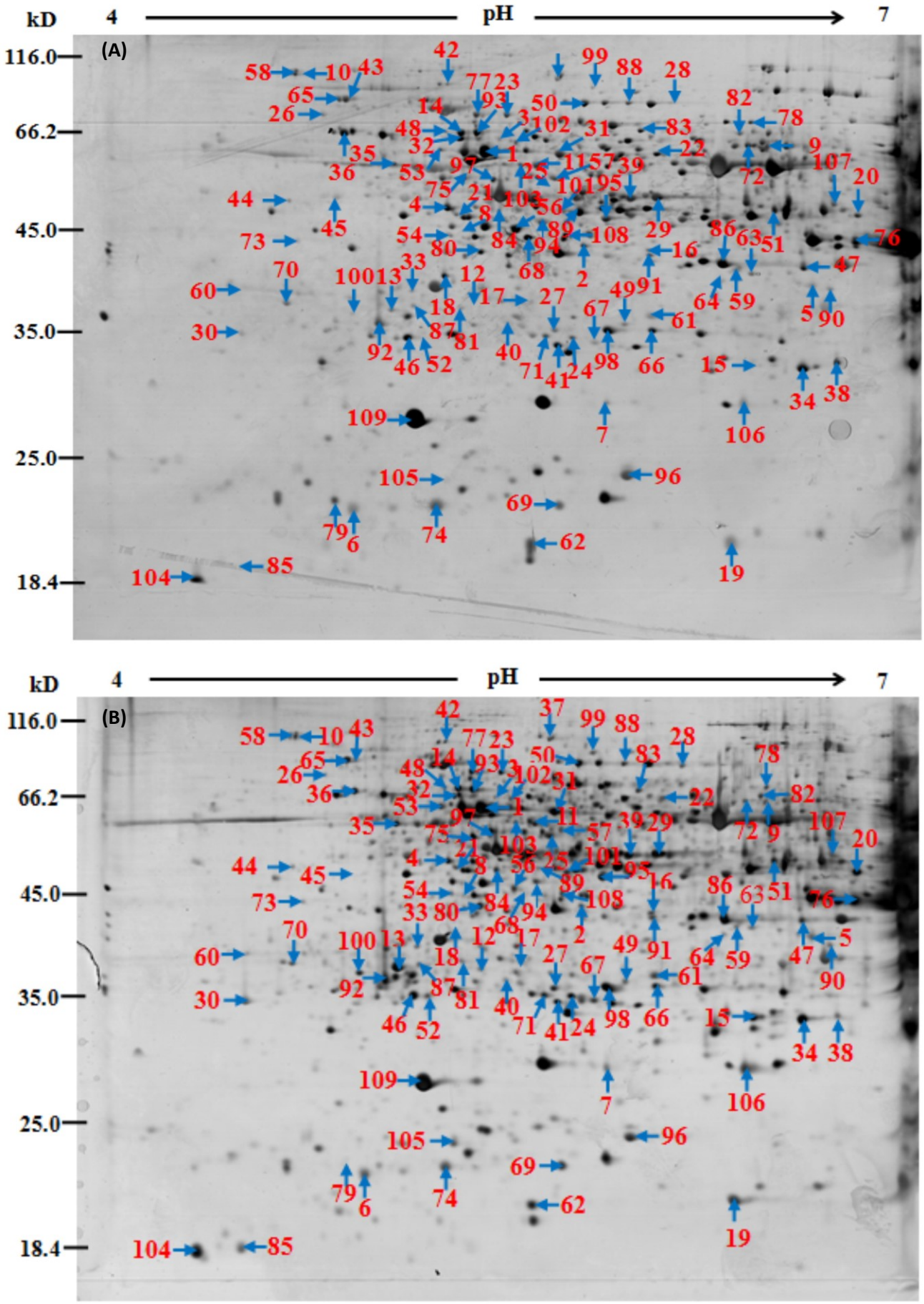

Fig. 1. 2D electrophoresis gels of extracts of roots under salt stress in cultivars JW9-6 (A) and JW2372 (B). The numbers with arrows represent the protein spots which were reliably identified.

Table 1. Proteins identified in roots of shrub willow clones with changed abundance under salt stress.

[a]Spot no.	[b]Uniprot no.	[c]Protein name	[d]Genename	[e]Protein score	[f]SC(%)	[g]MP	[h]0 h	2 h	12 h	72 h	0 h	2 h	12 h	72 h
1.	B9GH28	Mitochondrial processing peptidase	POPTR_0001s19190g	55	1	1	1.00	0.70	0.94	0.47*	1.00	2.01*	0.66*	0.71
2.	B9GYV3	Enoyl-Acp reductase 1	POPTR_0003s21820g	166	6	3	1.00	0.47*	1.05	2.46*	1.00	2.05*	1.78*	1.92*
3.	B9GMI8	Chaperonin Cpn60-2	POPTR_0001s14040g	160	5	2	1.00	0.34*	0.70	1.61*	1.00	2.48*	1.98*	2.72*
4.	A9PBT7	Putative adenosine kinase family protein	POPTR_0010s23120g	197	8	2	1.00	0.71	1.19	0.52*	1.00	1.28	0.55*	1.10
5.	B9H2K7	Malate dehydrogenase	POPTR_0004s05340g	297	10	2	1.00	1.00	1.06	2.73*	1.00	1.07	1.68*	1.15
6.	B9HQ83	Cytosolic ascorbate peroxidase	POPTR_0009s02070g	111	6	2	1.00	0.76	0.87	0.70	1.00	0.49*	0.29*	0.35*
7.	B9I056	Flavodoxin-like quinone reductase 1	POPTR_0011s13310g	99	7	1	1.00	1.05	0.70	1.76	1.00	0.76	1.25	0.48*
8.	B9MY45	PfkB-type carbohydrate kinase	POPTR_0017s05770g	212	15	4	1.00	0.79	1.08	1.51*	1.00	1.25	0.99	1.18
9.	B9HS53	D-3-phosphoglycerate dehydrogenase	POPTR_0009s09950g	100	4	2	1.00	1.40	2.03*	1.11	1.00	1.70*	0.91	1.16
10.	B9GV29	Glucose-6-phosphate isomerase	POPTR_0002s10420g	71	5	2	1.00	0.48*	0.43*	0.15*	1.00	1.53*	0.88	1.23
11.	B9HK35	Vacuolar ATP synthase catalytic subunit A	POPTR_0008s00560g	500	14	6	1.00	0.73	0.57*	0.64*	1.00	1.50*	1.04	0.95
12.	B9HJH4	Semialdehyde dehydrogenase	POPTR_0008s13510g	639	24	5	1.00	0.83	0.25*	0.97	1.00	1.40	1.03	1.27
13.	A9PGS6	O2 evolving complex 33kD	POPTR_0007s12070g	220	17	4	1.00	1.09	0.57*	0.68	1.00	1.13	0.59*	0.63*
14.	B9HWA2	ATP synthase subunit beta	POPTR_0010s12680g	232	9	3	1.00	0.87	0.92	1.03	1.00	1.05	0.63*	0.71
15.	B9I056	Flavodoxin-like quinone reductase 1	POPTR_0011s13310g	132	7	1	1.00	1.92*	1.65*	1.19	1.00	0.75	0.59*	0.42*
16.	B9HIJ5	Dihydrolipoyl dehydrogenase	POPTR_0008s10020g	67	12	1	1.00	0.64*	0.74	0.62*	1.00	1.48	1.34	1.90*
17.	B9HQ83	Cytosolic ascorbate peroxidase	POPTR_0009s02070g	79	6	1	1.00	1.36	0.72	3.80*	1.00	1.30	0.86	1.20
18.	B9HMD9	Uncharacterized protein	POPTR_0008s20770g	83	12	2	1.00	1.12	0.64*	0.76	1.00	1.18	2.17*	1.03
19.	A9PC26	Peroxiredoxin	POPTR_0001s44990g	82	12	2	1.00	0.11*	0.18*	0.09*	1.00	0.45*	0.11*	0.10*
20.	B9GTD8	Elongation factor Tu	POPTR_0002s22460g	112	7	2	1.00	4.14*	3.10*	2.18*	1.00	0.52*	0.59*	0.65*
21.	B9GZT5	Phosphoribulokinase	POPTR_0003s09830g	214	9	3	1.00	0.62*	1.12	1.28	1.00	1.11	0.79	0.94
22.	B9HS53	D-3-phosphoglycerate dehydrogenase	POPTR_0009s09950g	81	7	3	1.00	0.67	0.89	1.62*	1.00	1.56*	1.33	1.69*
23.	B9H8V2	Uncharacterized protein	POPTR_0006s15380g	93	6	3	1.00	0.91	0.76	0.86	1.00	0.86	0.59*	0.80
24.	B9INC6	20 kDa chaperonin	POPTR_0018s07410g	56	3	1	1.00	1.14	1.00	2.08*	1.00	1.33	0.72	0.84
25.	B9GH28	Mitochondrial processing peptidase	POPTR_0001s19190g	139	5	2	1.00	0.88	0.86	1.25	1.00	0.90	0.56*	0.95
26.	B9GU26	Protein disulfide-isomerase	POPTR_0002s08260g	110	4	2	1.00	0.96	0.56*	0.46*	1.00	6.09*	2.58*	1.96*
27.	A9PAG0	Proteasome subunit alpha type	POPTR_0012s14980g	163	9	2	1.00	0.56*	0.55*	1.38	1.00	1.59*	0.89	1.03
28.	B9GPE7	Transketolase	POPTR_0002s14730g	215	5	3	1.00	1.13	0.31*	0.49*	1.00	0.74	1.41	1.24
29.	A9PCR0	Malate dehydrogenase	POPTR_0011s09860g	220	8	3	1.00	0.78	0.90	0.45*	1.00	0.57	0.49*	0.61*
30.	B9H597	Uncharacterized protein	POPTR_0005s08480g	57	1	1	1.00	1.35	1.11	0.29*	1.00	2.20*	2.83*	1.83*
31.	A9PIJ2	Phosphopyruvate hydratase	POPTR_0006s11800g	182	6	2	1.00	0.80	0.81	0.48*	1.00	0.76	0.45*	0.78
32.	B9HN74	Heat shock protein 70	POPTR_0009s08320g	281	8	4	1.00	0.73	0.35*	0.44*	1.00	1.64*	0.92	1.45
33.	A9PE73	Chalcone-flavonone isomerase	POPTR_0010s21980g	161	10	3	1.00	0.89	1.08	1.64*	1.00	1.43	0.52*	0.70
34.	A9PCP4	Superoxide dismutase	POPTR_0019s08540g	98	9	2	1.00	1.10	1.15	0.68	1.00	0.73	0.40*	0.42*
35.	U5FHJ0	Uncharacterized protein	POPTR_0017s05330g	83	1	2	1.00	1.01	0.48*	0.61*	1.00	0.90	0.72	0.93
36.	B9MZ75	Rubisco subunit binding-protein alpha subunit	POPTR_0004s22340g	392	13	6	1.00	0.93	0.86	0.54*	1.00	0.75	0.50*	0.66*
37.	B9GPE7	Transketolase	POPTR_0002s14730g	138	9	4	1.00	0.80	0.37*	0.43*	1.00	1.33	0.71	0.98
38.	A9PIC8	Ribulose-phosphate 3-epimerase	POPTR_0001s34010g	127	10	2	1.00	1.27	1.90*	1.60*	1.00	0.54*	1.49	1.44
39.	B9HYU1	Leucoanthocyanidin reductase	POPTR_0011s03430g	59	4	1	1.00	0.69	1.46	0.44*	1.00	0.51*	0.40*	0.49*

Table 1. (Cont'd.)

[a]Spot no.	[b]Uniprot no.	[c]Protein name	[d]Genename	[e]Protein score	[f]SC(%)	[g]MP	[h]0 h	2 h	12 h	72 h	0 h	2 h	12 h	72 h
40.	A9PCS2	Eukaryotic translation initiation factor 3	POPTR_0010s19940g	171	12	2	1.00	1.35	0.85	2.84*	1.00	1.99*	0.70	1.15
41.	B9HSJ8	Ferritin	POPTR_0010s19190g	68	5	1	1.00	1.23	0.74	0.65*	1.00	1.44	0.90	0.93
42.	B9HN74	Heat shock protein 70	POPTR_0009s08320g	345	13	6	1.00	1.47	0.59*	0.91	1.00	1.41	2.27*	1.39
43.	B9HQD5	Rubisco subunit binding-protein alpha subunit	POPTR_0009s01470g	580	18	8	1.00	0.48*	0.69	0.33*	1.00	0.83	0.41*	0.49*
44.	A9PE95	Uncharacterized protein	POPTR_0008s10050g	116	8	3	1.00	1.04	0.55*	0.82	1.00	1.89	1.70	2.31*
45.	A9PF94	Sedoheptulose-1 family protein	POPTR_0010s20060g	374	14	5	1.00	0.89	1.14	1.42	1.00	0.96	0.54*	0.74
46.	B9GMZ5	DREPP plasma membrane polypeptide	POPTR_0001s12390g	91	6	1	1.00	1.03	0.94	1.03	1.00	1.28	0.69	0.62*
47.	B9GT82	Peroxidase	PRX17	69	4	1	1.00	1.63*	1.79*	1.60*	1.00	1.01	1.40	0.87
48.	A9PF58	Uncharacterized protein	POPTR_0001s03980g	464	16	7	1.00	4.04*	2.12*	2.47*	1.00	0.73	0.53*	0.45*
49.	A9P9I1	Proteasome subunit alpha type	POPTR_0016s14640g	80	9	2	1.00	0.94	0.56*	1.82*	1.00	1.35	1.06	1.44
50.	B9H3E2	Uncharacterized protein	POPTR_0004s08110g	245	8	4	1.00	0.57*	0.66*	0.60*	1.00	0.68	0.50*	0.81
51.	B9H088	Naregenin-chalcone synthase	POPTR_0003s17550g	159	8	3	1.00	1.85*	1.73*	1.18	1.00	0.92	0.69	0.98
52.	A9PFF7	Cysteine proteinase	POPTR_0014s02410g	223	6	2	1.00	1.51*	1.01	6.89*	1.00	1.45	0.76	1.23
53.	B9IA25	FtsH-like protein Pftf	POPTR_0014s13560g	55	2	2	1.00	0.46*	0.92	1.29	1.00	1.13	1.12	1.34
54.	A9P841	Pyruvate dehydrogenase	POPTR_0003s16480g	82	2	1	1.00	1.79*	1.83*	3.24*	1.00	1.28	1.16	0.73
55.	B9HYH4	Uncharacterized protein	POPTR_0010s18770g	73	4	2	1.00	1.96*	1.37	2.32*	1.00	2.28*	1.51*	2.02*
56.	B9HSR0	60S acidic ribosomal protein P0	POPTR_0010s19860g	100	12	2	1.00	1.30	1.56*	1.56*	1.00	1.64*	1.14	0.98
57.	A9PHC5	S-adenosylmethionine synthase 4	METK4	216	17	4	1.00	0.42*	0.63*	1.07	1.00	1.17	1.33	1.38
58.	A4GYR7	ATP synthase subunit beta, chloroplastic	AtpB	756	21	7	1.00	8.50*	8.02*	5.50*	1.00	0.73	1.34	0.87
59.	A9PBH3	Eukaryotic translation initiation factor 5A	POPTR_0008s09150g	229	26	4	1.00	1.25	1.16	3.19*	1.00	2.50*	2.80*	2.84*
60.	B9MY45	PfkB-type carbohydrate kinase	POPTR_0017s05770g	152	7	2	1.00	1.08	1.23	2.93*	1.00	3.84*	4.72*	4.75*
61.	B9HQ83	Cytosolic ascorbate peroxidase	POPTR_0009s02070g	131	9	2	1.00	0.56*	0.67*	1.16	1.00	1.06	0.56*	0.87
62.	B9HCW7	Pyridoxin biosynthesis PDX1-like protein 3	POPTR_0006s10130g	115	8	2	1.00	0.69	0.39*	0.46*	1.00	0.89	0.53*	1.45
63.	A9PB10	Glutamine synthetase	POPTR_0007s07960g	302	12	3	1.00	1.13	1.89*	4.75*	1.00	1.48	1.56*	1.55*
64.	A9PGB9	Leucoanthocyanidin reductase	POPTR_0004s03030g	50	4	1	1.00	0.86	0.76	4.94*	1.00	3.00*	2.40*	3.83*
65.	A9PHZ3	Vacuolar ATP synthase subunit B	POPTR_0004s18400g	77	8	3	1.00	0.51*	0.46*	0.25*	1.00	0.61*	0.58*	0.68
66.	A4GYR8	Ribulose bisphosphate carboxylase large chain	RbcL	312	9	4	1.00	0.82	0.86	1.34	1.00	1.63*	1.37	1.57*
67.	B9INC6	20 kDa chaperonin	POPTR_0018s07410g	70	5	2	1.00	0.89	1.37	3.55*	1.00	0.97	0.67	0.69
68.	A9PEP7	Uncharacterized protein	POPTR_0005s11600g	83	5	2	1.00	0.79	1.17	1.32	1.00	1.77*	2.09*	2.34*
69.	B9GXY1	Uncharacterized protein	POPTR_0003s20890g	419	19	5	1.00	0.73	0.78	0.96	1.00	1.21	0.64*	1.14
70.	A9P8D8	Uncharacterized protein	POPTR_0013s10250g	274	17	4	1.00	1.01	1.09	0.85	1.00	1.57*	1.60*	0.74
71.	A9PBH3	Eukaryotic translation initiation factor 5A	POPTR_0008s09150g	117	13	2	1.00	1.60*	1.40	2.90*	1.00	1.23	0.80	0.85
72.	B9H0I7	UDP-glucose 6-dehydrogenase	POPTR_0004s11760g	93	6	3	1.00	1.04	2.33*	1.38	1.00	1.40	1.13	1.38
73.	B9HH42	Uncharacterized protein	POPTR_0007s01850g	114	15	2	1.00	0.74	1.13	1.57*	1.00	1.92*	2.76*	1.90*
74.	A4GYR6	ATP synthase epsilon chain	AtpE	114	8	2	1.00	0.15*	0.71	0.13*	1.00	2.48*	0.35	0.39
75.	A9PBT7	Putative adenosine kinase	POPTR_0010s23120g	197	9	2	1.00	1.45	0.57*	0.66*	1.00	1.07	0.78	0.89
76.	A9PCR0	Malate dehydrogenase	POPTR_0011s09860g	424	11	4	1.00	1.76*	2.27*	1.33	1.00	0.76	1.21	0.63*
77.	B9GVR2	Uncharacterized protein	POPTR_0003s11300g	260	8	6	1.00	0.63*	0.66*	0.57*	1.00	0.79	0.51*	0.56*
78.	B9INY9	T-complex protein 1 subunit gamma	POPTR_0019s00210g	68	3	2	1.00	1.68*	1.71*	1.41	1.00	1.04	1.25	2.22*

Table 1. (Cont'd.)

[a]Spot no.	[b]Uniprot no.	[c]Protein name	[d]Genename	[e]Protein score	[f]SC(%)	[g]MP	[h]0 h	2 h	12 h	72 h	0 h	2 h	12 h	72 h
79.	B9N7I3	Proteasome subunit alpha type	POPTR_0001s16310g	58	9	1	1.00	0.98	1.06	1.26	1.00	2.55*	4.01*	3.53*
80.	B9H105	Glyoxalase I homolog family protein	POPTR_0004s01320g	51	4	1	1.00	1.41	1.06	1.44	1.00	1.29	0.78	0.84
81.	A9PHA9	O2 evolving complex 33kD	POPTR_0005s13860g	116	5	2	1.00	3.31*	1.17	10.08*	1.00	0.95	0.66*	1.04
82.	A9P8R3	Malate dehydrogenase	POPTR_0008s16670g	370	17	5	1.00	1.43	1.67*	1.23	1.00	1.31	1.23	1.46
83.	B9IGD0	Pyruvate decarboxylase	POPTR_0016s12760g	146	5	3	1.00	0.98	0.99	1.96*	1.00	0.36*	0.76	0.76
84.	B9HY30	Phosphoglycerate kinase	POPTR_0010s17870g	108	7	2	1.00	1.17	1.67	2.92*	1.00	1.85*	1.31	1.41
85.	B9H2K7	Malate dehydrogenase	POPTR_0004s05340g	131	6	2	1.00	1.54*	1.06	1.16	1.00	0.75	0.54*	1.75*
86.	B9N7N3	Nodule-enhanced malate dehydrogenase	POPTR_0004s11170g	308	9	5	1.00	0.67	0.89	0.50*	1.00	0.91	0.63*	0.53*
87.	B9HFI4	Fructose-bisphosphate aldolase	POPTR_0007s13800g	128	5	1	1.00	4.03*	2.51*	3.28*	1.00	1.46	0.86	1.27
88.	B9IGY9	Phosphoglycerate mutase	POPTR_0016s14950g	224	6	4	1.00	0.33*	0.36*	0.82	1.00	0.98	1.35	1.03
89.	B9N6N2	Type IIIa membrane protein cp-wap13	POPTR_0017s13350g	132	4	2	1.00	6.49*	6.33*	16.50*	1.00	2.01*	1.78*	2.01*
90.	A4GYR8	Ribulose bisphosphate carboxylase large chain	RbcL	113	7	2	1.00	1.04	0.97	0.98	1.00	0.95	1.41	1.92*
91.	O65904	Isoflavone reductase family protein	Pceberh	80	9	2	1.00	0.80	0.33*	1.52*	1.00	1.03	1.04	0.90
92.	B9GMZ5	DREPP plasma membrane polypeptide	POPTR_0001s12390g	68	6	1	1.00	0.56*	1.92*	0.66*	1.00	0.97	0.47*	2.04*
93.	B9GPE7	Transketolase family protein	POPTR_0002s14730g	118	8	3	1.00	0.83	1.00	0.65*	1.00	0.89	0.54*	0.70
94.	A9PEX7	Uncharacterized protein	THI1	72	3	1	1.00	0.91	0.52*	2.00*	1.00	1.48	0.87	1.17
95.	B9HY29	Phosphoglycerate kinase	POPTR_0010s17860g	421	14	5	1.00	0.85	1.54*	0.97	1.00	0.85	0.69	0.48*
96.	A4GYR8	Ribulose bisphosphate carboxylase large chain	RbcL	366	7	5	1.00	0.32*	0.87	0.15*	1.00	0.40*	0.52*	0.24*
97.	B9HI53	Phosphoglycerate kinase	POPTR_0008s08410g	142	3	1	1.00	0.88	1.16	0.72	1.00	1.73*	1.41	0.94
98.	B9GKN8	Elongation factor Tu	POPTR_0001s08770g	171	5	2	1.00	0.75	1.04	0.65*	1.00	1.42	0.94	0.76
99.	B9GSZ3	S-adenosylmethionine synthase	POPTR_0002s19000g	107	18	2	1.00	1.21	0.69	4.07*	1.00	1.00	1.17	1.65*
100.	B9MY45	PfkB-type carbohydrate kinase	POPTR_0017s05770g	163	8	2	1.00	2.32*	1.22	1.40	1.00	1.35	0.79	0.68
101.	B9I4S5	Glutamine synthetase	POPTR_0012s04090g	133	18	2	1.00	1.30	1.51*	1.97*	1.00	0.91	1.07	1.11
102.	B9GMI8	Chaperonin CPN60-2	POPTR_0001s14040g	145	4	3	1.00	1.00	0.99	1.32	1.00	1.04	0.62*	0.71
103.	A9P830	Caffeic acid 3-O-methyltransferase	COMT1	302	16	5	1.00	1.65*	0.63*	2.12*	1.00	2.24*	1.42	1.21
104.	A9PG34	Plastocyanin family protein	POPTR_0002s01740g	73	12	1	1.00	0.57*	0.68	1.26	1.00	0.95	2.77*	1.04
105.	A9PGS6	O2 evolving complex 33kD	POPTR_0007s12070g	125	6	1	1.00	0.19*	0.29*	0.16*	1.00	1.02	0.86	0.52*
106.	A9PGP9	Oxygen-evolving complex protein	POPTR_0002s05660g	117	9	2	1.00	0.97	1.26	1.54*	1.00	0.50*	0.33*	0.25*
107.	B9H5U1	Glyceraldehyde-3-phosphate dehydrogenase	POPTR_0005s27550g	58	7	2	1.00	1.27	3.10*	1.93*	1.00	0.44*	0.94	1.04
108.	A9PI59	Glyceraldehyde-3-phosphate dehydrogenase	POPTR_0014s13660g	135	12	3	1.00	0.77	1.38	1.81*	1.00	2.05*	2.15*	2.08*

[a] Numbering corresponds to the 2-DE in Fig. 1

[b] Accession number from the Uniprot database

[c] Names of the proteins obtained via the MASCOT software from the Uniprot database

[d] Genenames from the Uniprot database

[e] MOWSE score probability for the entire protein

[f] The sequence coverage of identified proteins

[g] The total number of identified peptide

[h] The protein abundance ratio (Treatment/Control) at each particular time point

* Indicates significant (more than 1.5-fold or less than 0.66-fold) difference between control and treatment at 0.05 level

Functional analysis of identified proteins: A total of 67 identified proteins (61.5% in total) in response to salt stress were obviously classified into eight functional categories, including energy metabolism, stress and defense, redox homeostasis, proteolytic proteins, protein synthesis, protein folding and assembly, amino acid and nitrogen metabolism, and secondary metabolism (Fig. 2). Most of these proteins (47.7%) implicated in energy metabolism, and changed larger in JW9-6 (salt-sensitive) than JW2372 (salt-tolerant). After salt stress, proteins involved in protein metabolism including proteolytic proteins, protein synthesis, protein folding and assembly, were more up-regulated in JW2372 (salt-tolerant) than in JW9-6 (salt-sensitive). Furthermore, the proteins which were reliably identified, were analyzed using DAVID toolkit, in an effort to inquiry functional information involved in metabolic pathways. On the one hand, the functional enrichment of 91 differentially expressed proteins from cultivar JW9-6 (salt-sensitive) in biological process (BP), cellular component (CC), and molecular function (MF) categories by gene ontology (GO) analysis, respectively, were displayed in Fig. 3(A). In the BP analysis, the majority of identified proteins were grouped into metabolic process, especially in purine ribonucleoside, purine nucleoside, ribonucleoside, purine-containing compound, nucleoside, and glycosyl compound metabolic process, which each accounted for 16.4%. The CC analysis indicated that most of identified proteins were classified into cytoplasm which accounted for 36.8%. Molecular functional classification of identified proteins revealed that most participated in coenzyme and cofactor binding, which each accounted for 10.6%. On the other hand, the functional enrichment of 78 identified proteins from JW2372 (salt-tolerance) in biological process (BP), cellular component (CC), and molecular function (MF) categories by gene ontology (GO) analysis, respectively , were displayed in Fig. 3(B). The BP analysis showed that protein folding, which accounted for 13.1%, was the most group. In the CC analysis, the most of identified proteins were classified into cell and cell part, which each accounted for 48.4%. The third group of these proteins belonged to cell periphery which accounted for 18.1%. Molecular functional classification of 78 proteins revealed that most participated in isomerase activity and coenzyme binding, which each accounted for 15.4%. Coenzyme binding was also found in the MF process from identified proteins in cultivar JW9-6 (salt-sensitive).

The results from comparison of GO analysis in shrub willow clones indicated that the majority functions including BP (metabolic process and protein folding), CC (cytoplasm and cell) and MF (cofactor, coenzyme binding and isomerase activity), regulated by root proteins, were differences between JW2372 (salt-tolerance) and JW9-6 (salt-sensitive) under salinity stress. These differences may be one of the reasons that JW2372 is more salt tolerant than JW9-6. Shrub willow clones proteins-involved in salinity showed kinds of cellular distributions and functions, compatible with the fact that salinity, the stress factor, participated in multiple indispensable activities via its interaction with the components of shrub willow clones roots.

Pathway enrichment of differentially expressed proteins: To gain the change of pathways affacted by differentially expressed proteins, KEGG pathway analysis was executed using Omicsbean software (Du *et al.,* 2016). The results of KEGG pathway enrichment revealed that these proteins were mainly related in glyoxylate and dicarboxylate metabolism, pyruvate metabolism, glycolysis, ascorbate and aldarate metabolism, amino sugar and nucleotide sugar metabolism, pentose phosphate pathway, and cysteine and methionine metabolism. Among the seven pathways, glyoxylate and dicarboxylate metabolism have the highest score and lowest E value. Analsis results also showed that 23 proteins from *Populus trichocarpa* participate in glyoxylate and dicarboxylate metabolism, but only four of them changed their expression after salt stress (Fig. 4.). The four proteins which labeled in blue circles in Fig. 4., were identified from nine spots (5, 16, 29, 63, 66, 85, 90, 96 and 109), because of numerous factors, such as different gene expression products, expression in different organisms, or post-translational modifications of the same gene expression. Four spots (5, 16, 63 and 85) increased their expression and three spots (29, 96 and 109) decreased their expression after salt stress in both cultivars, but two spots (66 and 90) were up-regulated by salt stress only in salt-tolerance cultivar JW2372. This phenomenon indicated that shrub willow clones increased its resistance to the salinity by up-regulating glyoxylate and dicarboxylate metabolism, and acceleration of glyoxylate and dicarboxylate metabolism may be one of the reasons that cultivar JW2372 is more salt tolerant than cultivar JW9-6.

In the same way, on the basis of difference from proteins involved in other six pathways, we found that (1) the pyruvate metabolism regulated by seven proteins (5, 16, 28, 30, 56, 76 and 85), were enhanced stronger in cultivar JW2372 than cultivar JW9-6; (2) the pathway of glycolysis regulated by five proteins (10, 16, 83, 84 and 88), were decreased in cultivar JW2372 but increased in cultivar JW9-6; (3) the ascorbate and aldarate metabolism regulated by six proteins (6, 13, 17, 61, 72 and 105), were decreased lower in cultivar JW9-6 than cultivar JW2372; (4) the amino sugar and nucleotide sugar metabolism regulated by seven proteins (8, 10, 60, 72, 73, 89 and 100), were enhanced stronger in cultivar JW2372 than cultivar JW9-6; (5) the pentose phosphate pathway regulated by four proteins (10, 28, 37 and 93), were decreased lower in cultivar JW2372 than cultivar JW9-6; (6) the cysteine and methionine metabolism regulated by seven proteins (5, 12, 29, 56, 76, 85 and 99), were enhanced stronger in cultivar JW2372 than cultivar JW9-6. On the base of the above, we guessed that the changing of these pathways were the main reasons why JW2372 have more salt tolerance than JW9-6.

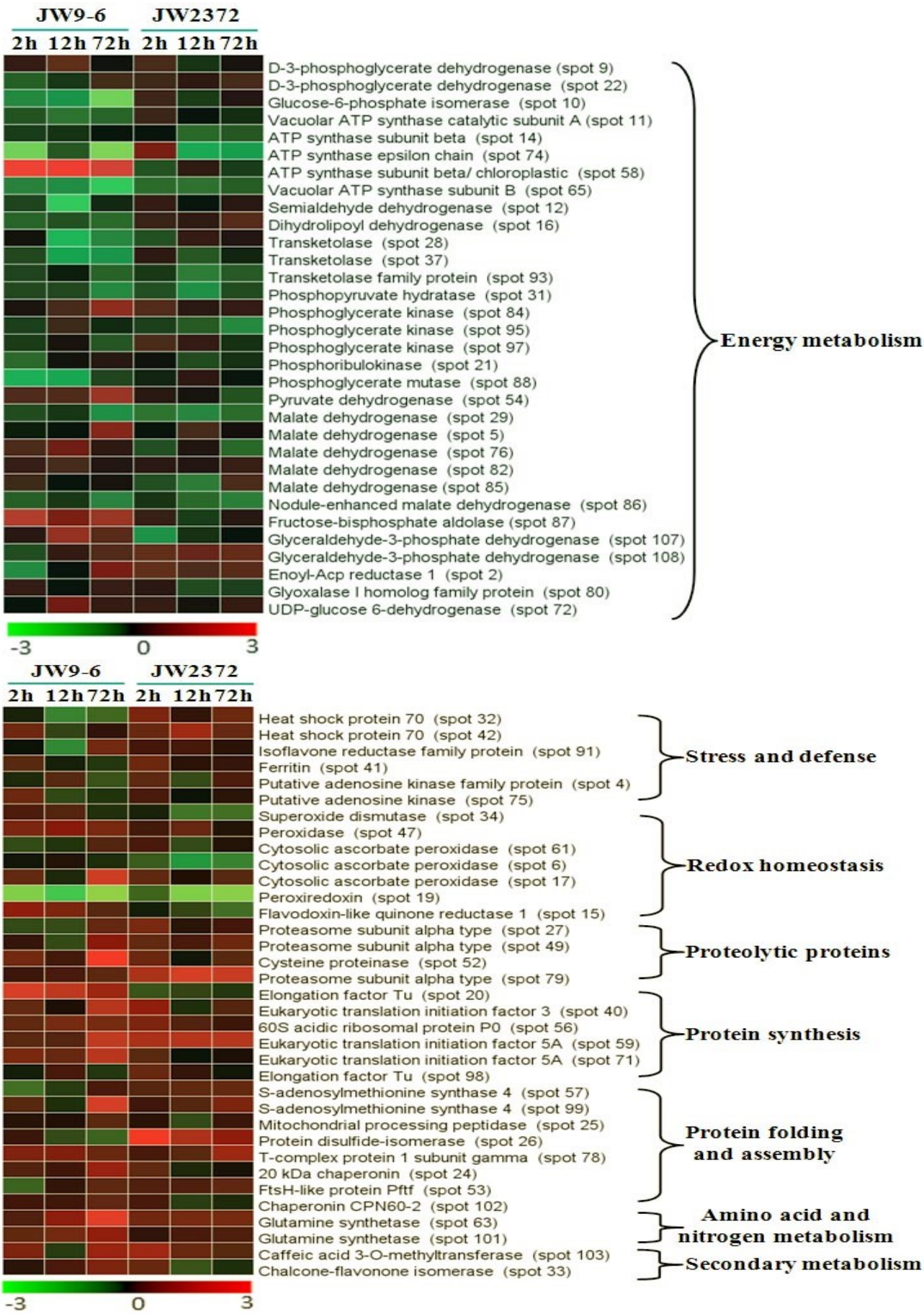

Fig. 2. Hierarchical clustering of salt-responsive proteins in both varieties JW2372 (salt-tolerant) and JW9-6 (salt-sensitive).

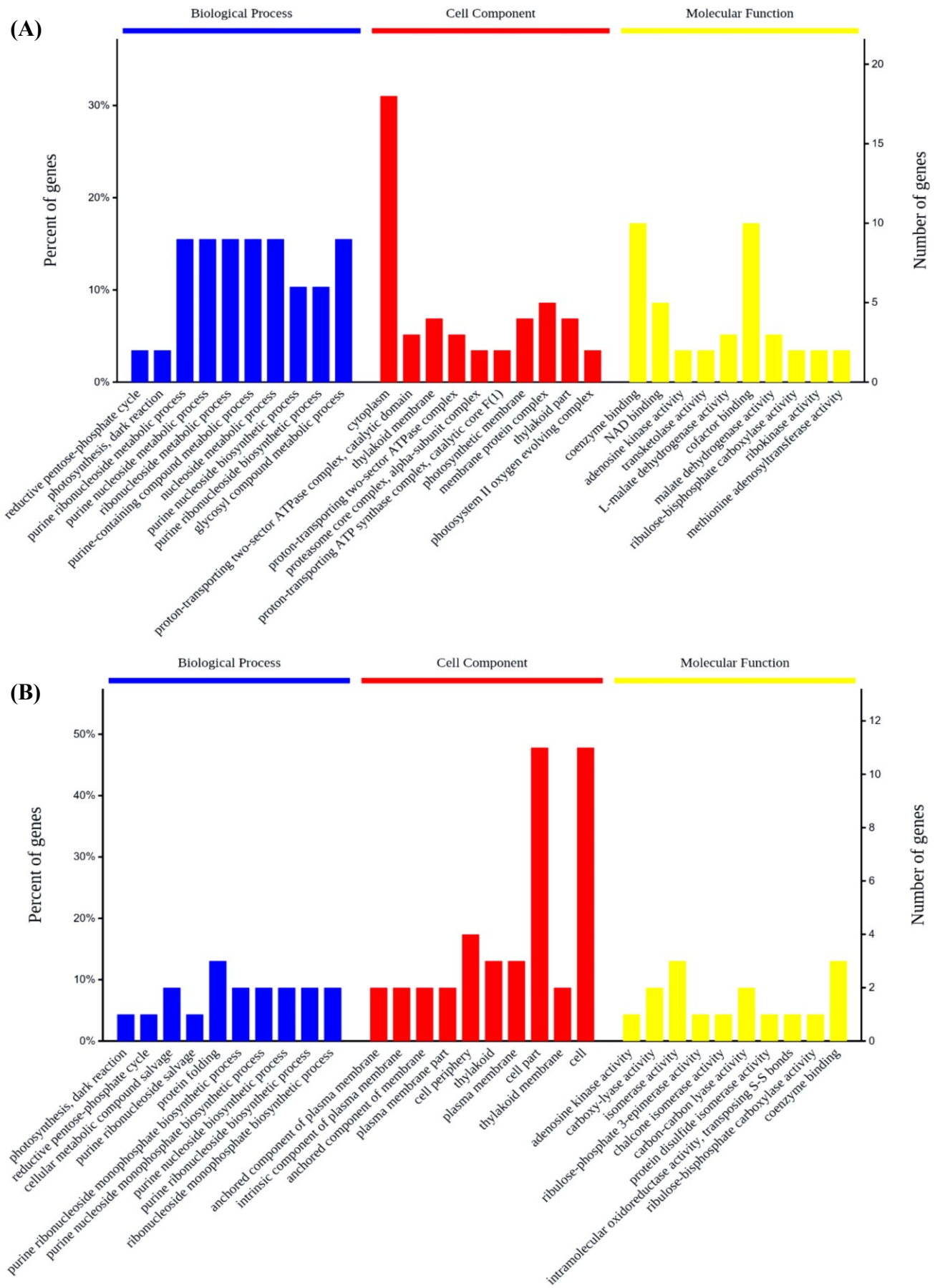

Fig. 3. GO annotation of identified shrub willow clones proteins-related to salinity in three categories: biological process (BP), cellular component (CC) and molecular function (MF). (A): Enrichment of GO from cultivar JW9-6 (salt-sensitive); (B): Enrichment of GO from cultivar JW2372 (salt-tolerance).

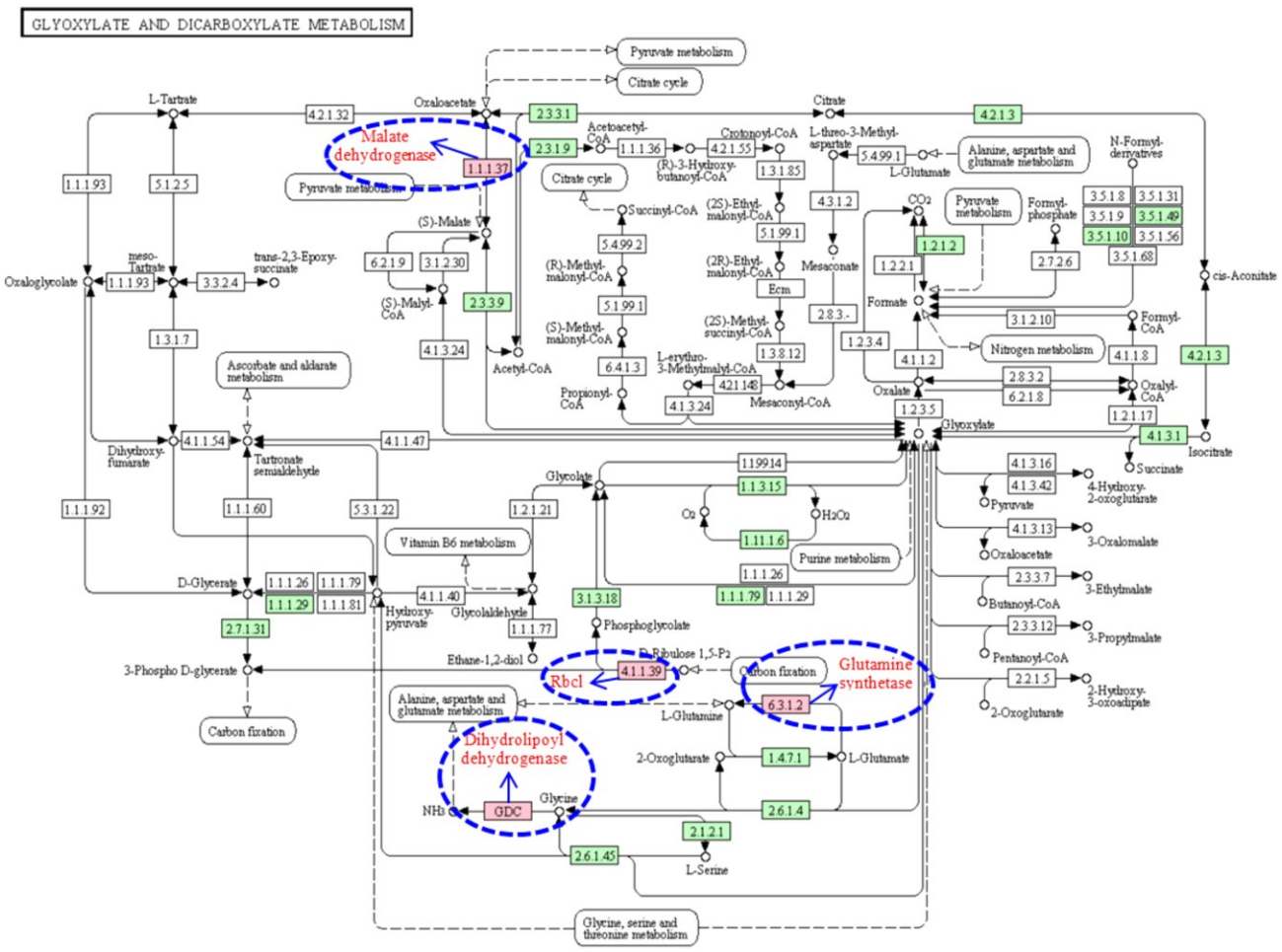

Fig. 4. Significantly enriched glyoxylate and dicarboxylate metabolism pathway. Four proteins labeled in blue circles were identified by MALDI-TOF-TOF MS in the present study. The green color represents other proteins from *Populus trichocarpa* in this pathway.

Networks of protein-protein interaction from differentially expressed proteins: To further inquiry relevant information from the identified proteins, a more comprehensive bioinformatics analysis of the proteomics data was performed using Cytoscape, a powerful tool for integrating protein-protein interaction (PPI) networks into a unified conceptual framework (Zhang *et al.,* 2014; Xu *et al.,* 2015). Again, PPI analysis showed that purine ribonucleoside metabolic process as the most significantly enriched pathways indicated in Fig. 5A, and carbon metabolism, purine ribonucleoside biosynthetic process, and purine nucleoside biosynthetic process in Fig. 5B.Further analysis, we can see that four important genes (METK4, POPTR_0010s23120g, POPTR_0010s17870g and POPTR_0002s10420g) have interaction with purine ribonucleoside metabolic process, and two important genes (atpE and POPTR_0010s23120g) have interaction with both purine ribonucleoside biosynthetic process, and purine nucleoside biosynthetic process. Gene POPTR_0010s23120g appeared in both PPI networks. Among of the five genes/ proteins, POPTR_0002s10420g/ glucose-6-phosphate isomerase and atpE/ ATP synthase epsilon chain decreased their expression after salt stress in salt-sensitivecultivar JW9-6, but increased their expression after salt stress in salt-tolerance cultivar JW2372. POPTR_0010s17870g/ phosphoglycerate kinase was up-regulated by salt stress in both cultivars. The last two genes/proteins, METK4/ S-adenosylmethionine synthase 4 and POPTR_0010s23120g/ adenosine kinase, decreased their expression after salt stress only in salt-sensitivecultivar JW9-6. From the expression differences of five genes/proteins between salt-sensitivecultivar JW9-6 and salt-tolerance cultivar JW2372, and the pathways involved in five genes/proteins, we guessed that the five genes/proteins have the key roles in the process of resisting salt stress in plants. Therefore, five proteins, glucose-6-phosphate isomerase, ATP synthase epsilon chain, phosphoglycerate kinase, S-adenosylmethionine synthase 4 and adenosine kinase, could be candidate proteins for plant breeding associated with salt stress. The discovery of five proteins supply an important train of thought and help for research of molecular mechanism related to salt stress in plants.

In recent years, the study of proteomics has provided us with a better understanding of the regulatory mechanisms of plants, animals and microorganisms (Jiang *et al.,* 2007). We studied the effects of salt stress on the total protein expression of Shurb Willow roots by proteomic method. A total of 106 differentially expressed proteins were identified by MALDI-TOF-TOF MS. These proteins are involved pr

imarily in energy metabolism, stress and defense, redox homeostasis, proteolytic proteins, protein synthesis, protein folding and assembly, amino acid and nitrogen metabolism and secondary metabolism.The following will discuss the functions of differentially expressed proteins response to salt stress in Shurb Willow roots.

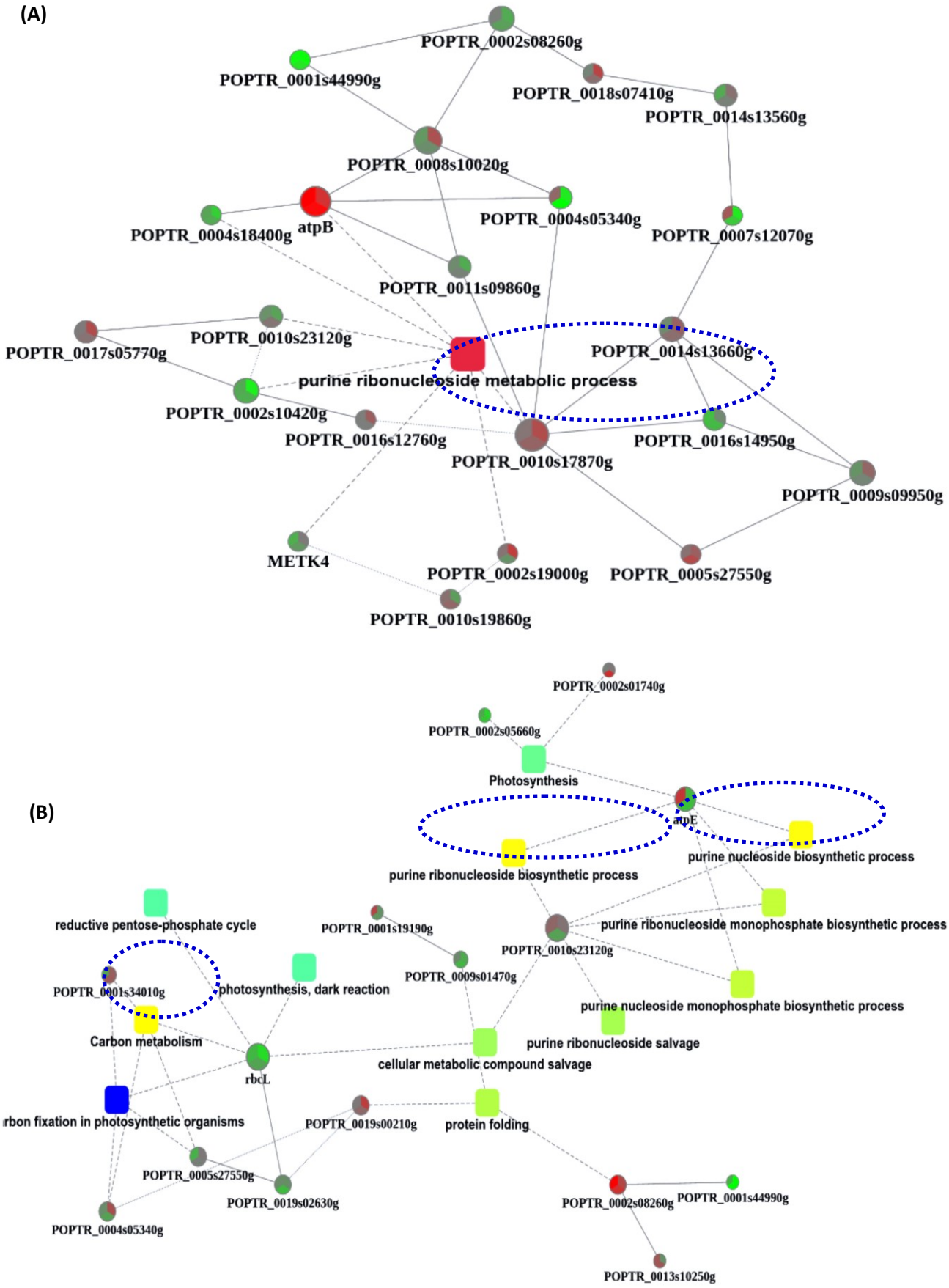

Fig. 5. A network of protein-protein interaction (PPI). The PPI analysis was based on fold change of protein/gene, protein-protein interaction, KEGG pathway enrichment and biological process enrichment. Circle nodes refer to proteins/genes, and rectangle refers to KEGG pathway or biological process, which were colored with gradient color from yellow (smaller *p*-value) to blue (bigger *p*-value). (A): PPI network of proteins from cultivar JW9-6 (salt-sensitive); (B): PPI network of proteins from cultivar JW2372 (salt-tolerance).

Discussion

Proteins involved in energy metabolism: Energy metabolism, is one of the most basic features of plant growth. A total of thirty-two proteins related to energy including glycolysis, carboxylic acid cycle and pentose phosphate pathway, were identified in our study. Among them, protein spots 11, 14, 74 and 58 are ATP synthases or their different subunits. ATP synthase is widely distributed in mitochondria, chloroplasts, prokaryotic algae, heterotrophic bacteria and photosynthetic bacteria (Wan *et al.,* 2008). Most of the ATP synthases in susceptible cultivar JW9-6 were down-regulated by salt stress, but no significant difference in salt tolerant cultivar JW2372. Spots 28 and 37 were identified as transketolases which involved in pentose phosphate pathway. The pentose phosphate pathway plays an important role in the Calvin cycle in plant photosynthesis (Wang *et al.,* 2015). In the salt-sensitive cultivar JW9-6 after salt stress for 12 hours and 72 hours, transketolase expressed decreased, but no differences in the salt-tolerant cultivar JW2372 under salt stress treatment. The supply of energy was restrained in cultivar JW9-6 may be one of the reasons why cultivar JW2372 has more salt tolerance than cultivar JW9-6. Protein spots 5, 76, 82, 84 and 85 are malate dehydrogenase which is enzyme regulating in the three carboxylic acid cycle. Because of the different sources of the enzyme, some of its properties are not the same proteins. In the experiment, malate dehydrogenase were down-regulated after salt stress in both varieties. This results showed that energy metabolism was weakened strongly by salt stress in Shurb Willow roots, and the growth of roots may be inhibited severely.

Proteins related to stress and defense: Plants have developed defense responses to abiotic and biotic stresses over evolutionary time as a survival mechanism (Katja *et al.,* 2009). Two proteins (spots 32 and 42) are heat shock proteins70 which is an evolutionarily highly conserved protein, with a variety of biological functions, including molecular chaperone, immune regulation, as well as in virus infection and defense (Zhang *et al.,* 2011). All kinds of organisms by external adverse or detrimental factors stimulation, will produce a physiological regulation of expression during this period, and some of the normal proteins in cells is inhibited or activated and expression. In this experiment, the expression of heat shock protein 70 was down-regulated after salt stress for 2 and 12 hours in cultivar JW9-6, but up-regulated in cultivar JW2372. The results indicated that Shurb Willow roots after salt stimulation in earlier stage started-up the defense signal to resist aggrieve by environmental factors. The defense signal was started-up more quickly in cultivar JW2372 than cultivar JW9-6 may be results in different from salt tolerance between two Shurb Willow cultivars. Other proteins related to stress and defense also have the similar expression trends in our study.

Redox homeostasis was out-of-balance in Shurb Willow roots after salt stress: Previous results showed that proteins associated with redox homeostasis during plant growth are changed by salt stress, including ascorbate peroxidase, GST, etc (Zheng *et al.,* 2012). In this experiment，spot 47 was identified as peroxidase, which was a kind of oxidoreductase produced by microorganisms or plants. Peroxidase could catalyze the oxidation of substrates with hydrogen peroxide as electron acceptor. Mainly in the peroxisomes, with iron porphyrin prosthetic group, can catalyze hydrogen peroxide, oxidation of phenol and amine compounds, which can eliminate the dual role of hydrogen peroxide and amine toxicity (Wang *et al.,* 2014). In sensitive cultivar JW9-6, the expression of peroxidasewas up-regulated after salt stress for 2 hours; while in salt-tolerant cultivar JW2372, peroxidase showed no significant difference under salt stress treatment. The other protein peroxiredoxin (spot 19) which is also related to redox homeostasis, is decreased its expression after salt stress in both cultivars. The above results indicated that redox homeostasis was out-of-balance in Shurb Willow roots after salt stress, and salt stress could inhibited plant growth via disturbing the balance of redox homeostasis.

Protein metabolism was disturbed in Shurb Willow roots after salt stress: Protein metabolism, the balance between synthesis and degradation, is one of many forms of regulation that are coordinated to achieve a unified cellular response to developmental and environmental cues (Wu *et al.,* 2016). It have three processes including the hydrolysis of proteins, folding and assembly, and the synthesis of proteins. Proteasome is a ATP dependent proteolytic complex composed of 20S catalytic particles, 11S regulatory factors and 19S regulatory particles (Zheng *et al.,* 2012). The active state of proteasome is very important for the maintenance of protein metabolism. In this experiment, spots 27、49 and 79 are proteasome subunit alpha type, and their expression was down regulated after salt stress in susceptible variety JW9-6, but up-regulated in salt tolerant cultivar JW2372. This is indicated that hydrolysis of proteins is enhanced by salt stress in salt tolerant cultivar JW2372. Otherwise, elongation factor could promote polypeptide chain elongation during mRNA translation (Li *et al.,* 2015). Spot 20 was identified as elongation factor Tu, which mediated aminoacyl -tRNA into the ribosome vacated position A. The "carry" process needs to consume EF-Tu to hydrolyze energy generated by its complex ATP (Li *et al.,* 2015). In Shurb Willow roots, the expression of elongation factor Tu was down-regulated by salt stress in susceptible variety JW9-6, but up-regulated in salt tolerant cultivar JW2372. The results showed that the synthesis of proteins was enhanced in salt tolerant cultivar JW2372, but inhibited in susceptible variety JW9-6. Two proteins are disulfide isomerase folding enzymes, which contain five domains, and was combined with protein folding (Ma *et al.,* 2014). In the experiment, disulfide-isomerase increased its expression in salt tolerant cultivar JW2372, but decreased its expression in susceptible variety JW9-6 after salt stress. This results suggested that process of protein folding and assembly was more stronger in salt tolerant cultivar JW2372 than in susceptible variety JW9-6 after salt stress. In summary, protein metabolism was disturbed in Shurb Willow roots after salt stress, and these proteins may be the key proteins in response to salt stress in Shurb Willow roots.

Differences from the salt-responsive pathways between leaves and roots in the shrub willow clones: To cope with salt stress, shrub willow clones have evolved complex salt-responsive signaling and metabolic pathways at the cellular and whole-plant levels (Zhu, 2001; Nam *et al.,* 2012). Conjoint analysis of the comparative proteomics results of both the seedling roots and leaves of shrub willow clones may be more helpful in understanding how it cope with salt stress at the whole-plant level (Aghaei & Komatsu, 2013). In the our study, our comparative proteomics analysis of shrub willow clones roots, combined with our previous comparative proteomics analysis of shrub willow clones leaves (Sui *et al.,* 2015), can provide a systematical comparison between the proteins involved in metabolic pathways found in shrub willow clones leaves and roots under salt stress. The main differences of the pathways were as follows: shrub willow leaves increases salt tolerance by enhancing its ROS scavenging capacity and protein proteolysis; inhibition of protein synthesis as well as folding and assembly; changing photosynthesis, carbohydrate metabolism, energy supply, and nitrogen and amino acid metabolism. But shrub willow roots increases salt tolerance by enhancing its pyruvate metabolism, amino sugar and nucleotide sugar metabolism, cysteine and methionine metabolism; inhibition of pathway of glycolysis, ascorbate and aldarate metabolism, and pentose phosphate pathway. Based on the comparative proteomics results of shrub willow leaves and roots, we can understand clearly mechanism of salt tolerance from shrub willow, and providing an important strategy for forest tree breeding involved in salt tolerance.

Conclusions

In this study, to investigate changes of total proteins under salinity stress, we performed a comparative proteome analysis of the seedling roots of two shrub willow clones (salt tolerant cultivar JW2372 and salt sensitive cultivar JW9-6) under salt stress. A total of 124 protein spots showed a more than 1.5-fold or less than 0.66-fold difference (p<0.05) in expression values in at least one salt stress time point compared to the control. 109 differentially expressed proteins were successfully identified by MALDI-TOF-TOF MS (Table 1).

By analyzing and camparing functions of the differentially expressed proteins, we obtained the conclusions as follows: 1) the majority functions including BP (metabolic process and protein folding), CC (cytoplasm and cell) and MF (cofactor, coenzyme binding and isomerase activity), regulated by root proteins, were differences between JW9-6 (salt-sensitive) and JW2372 (salt-tolerance) under salt stress; 2) six pathways were changed by salt stress, including pyruvate metabolism, glycolysis, ascorbate and aldarate metabolism, amino sugar and nucleotide sugar metabolism, pentose phosphate pathway, and cysteine and methionine metabolism; 3) analysis of PPI indicated that the five proteins including glucose-6-phosphate isomerase, ATP synthase epsilon chain, phosphoglycerate kinase, S-adenosylmethionine synthase 4 and adenosine kinase, could be candidate proteins for plant breeding associated with salt stress; 4) differences from the salt-responsive pathways between leaves and roots in the shrub willow clones could provide an important strategy for forest tree breeding involved in salt tolerance.

Such a mechanism at proteomic level allows us to understand clearly and describe the possible management strategy of cellular activities occurring in salt-treated shrub willow clones and provides an important train of thought and help for research of molecular mechanism related to salt stress in shrub willow.

Acknowledgments

This work was supported by the Science and Technology Support Program of Jiangsu Province (Grant No. BE2013449).

References

Aghaei, K. and S. Komatsu. 2013. Crop and medicinal plants proteomics in response to salt stress. *Front Plant Sci.,* 4: 1-9.

Bernstein, N. and A. Meiri. 2004. Root growth of avocado is more sensitive to salinity than shoot growth. *J. Am. Soc. Hort. Sci.,* 129: 188-192.

Bradford, M. 1976. A rapid and sensitive method for the quantitation of microgram quantities of protein utilizing the principle of protein-dye binding. *Anal. Biochem.,* 72: 248-254.

Du, D.F., X. Gao, J. Gong, Q.Y. Li, L.Q. Li and Q. Lv. 2016. Identification of key proteins and networks related to grain development in wheat (*Triticum aestivum* L.) by comparative transcription and proteomic analysis of allelic variants in TaGW2-6A. *Frontiers in Plant Science*, http://dx.doi.org/10.3389/fpls.2016.00922.

Espartero, J.J.A., T. Pintor and J.M. Pardo. 1994. Differential accumulation of S-adenosylmethionine synthetase transcripts in response to salt stress. *Plant Mol. Biol.,* 25: 217-227.

Jiang, Y.Q., B. Yang, N.S. Harris and M.K. Deyholos. 2007. Comparative proteomic analysis of NaCl stress-responsive proteins in Arabidopsis roots. *J. Exp. Bot.,* 13(58): 3591-3607.

Katja, W., A. Weidner, G.K. Surabhi, A. Borner and H.P. Mock. 2009. Salt stress-induced alterations in the root proteome of barley genotypes with contrasting response towards salinity. *J. Exp. Bot.,* 60(12): 3545-3557.

Li, W., F.A. Zhao, W.P. Fang, D.Y. Xie, J.N. Hou, X.J. Yang, Y.M. Zhao, Z.J. Tang, L.H. Nie and S.P. Lv. 2015. Identification of early salt stress responsive proteins in seedling roots of upland cotton (*Gossypium hirsutum* L.) employing iTRAQ-based proteomic technique. *Front. in Plant Sci.,* 6: 1-14.

Luo, Q.Y., B.J. Yu and Y.L. Liu. 2005. Differential sensitivity to chloride and sodiumions in seedlings of Glycine max and *G. soja* under NaCl stress. *J. Plant Physiol.,* 162: 1003-1012.

Ma, H.Y., L.R. Song, Z.G. Huang, Y. Yang, S. Wang, Z.K. Wang, J.H. Tong, W.H. Gu, H. Ma and L.T. Xiao. 2014. Comparative proteomic analysis reveals molecular mechanism of seedling roots of different salt tolerant soybean genotypes in responses to saliniby stess. *Eupa Open Proteomics,* 4: 40-57.

Ma, H.Y., L.R. Song, Y.J. Shu, S. Wang, J. Niu, Z.K. Wang, T. Yu, W.H. Gu and H. Ma. 2012. Comparative proteomic analysis of seedling leaves of different salt tolerant soybean genotypes. *J. Proteomics.,* 75: 1529-1546.

Nam, M.H., S.M. Huh, K.M. Kim, W.J. Park, J.B. Seo and K. Cho. 2012. Comparative proteomic analysis of early salt stress-responsive proteins in roots of SnRK2 transgenic rice. *Protein Sci.,* 25: 1-19.

Parker, H.Y., T.J. Flowers, A.L. Moore and N.V.J. Harpharm. 2006. An accurate and reproducible method for proteome profiling of the effects of salt stress in the rice leaf lamina. *J. Exp. Bot.,* 57: 1109-1118.

Sui, D.Z., B.S. Wang, S.Z. Shi and X.D. He. 2015. Changes of protein expression during leaves of shrub willow clones in response to salt stress. *Acta Physiol. Plant.,* 3: 37-51.

Sui, D.Z., B.S. Wang, S.Z. Shi and Z.Y. Jiao. 2011. Selection of identification index and comprehensive evaluation of salt tolerance at seedling stage of shrub willow clones. *J. Northwest For. Univ.,* 26: 61-64.

Sun, N.N., W.C. Sun, S.M. Li, J.B. Yang, L.F. Yang, G.H. Quan, X. Gao, Z.J. Wang, X. Cheng, Z.H. Li, Q.S. Peng and N. Liu. 2015. Proteomic analysis of cellular proteins Co-Immunoprecipitated with Nucleoprotein of influenza A Virus (H7N9). *Int. J. Mol. Sci.,* 16: 25982-25998.

Tang, W.Q., Z.P. Deng, A. Oses-Prieto, S. Nagi, S.W. Zhu and X. Zhang. 2008. Proteomic studies of brassinosteroid signal transduction using prefractionation and two-dimensional DIGE. *Mol. Cell Proteomic.,* 7: 728-738.

Wang, L.X., D.Z. Pan, J. Li, F.L. Tan, S.H. Benning, W.Y. Liang and W. Chen. 2015. Proteomic analysis of changes in the Kandelia candel chloroplastproteins reveals pathways associated with salt tolerance. *Plant Sci.,* 231: 159-172.

Wang, W., B. Vinocur and A. Altman. 2003. Plant responses to drought, salinity and extreme temperatures: towards genetic engineering for stress tolerance. *Planta,* 218: 1-14.

Wan, X.Y. and J.Y. Liu. 2008. Comparative proteomics analysis reveals an intimate protein network provoked by hydrogen peroxide stress in rice seedling leaves. *Mol. Cell Proteomic,* 7: 1469-1488.

Wang, Z.Q., X.Y. Xu, Q.Q. Gong, C. Xie, W. Fan, J.L. Yang, Q.S. Lin and S.J. Zheng. 2014. Root proteome of rice studied by iTRAQ provides integrated insight into aluminum stress tolerance mechanisms in plants. *J. Proteomics,* 98: 189-205.

Wu, L.J., L. Tian, S.X. Wang, J. Zhang, P. Liu, Z.Q. Tian, H.M. Zhang, H.P. Liu and Y.H. Chen. 2016. Comparative proteomic analysis of the response of maize (*Zea mays* L.) leaves to long photoperiod condition. *Front. in Plant Sci.,* 7: 1-16.

Xu, D.D., Y.Y. Li, X. Li, L.L. Wei, Z.F. Pan, T.T. Jiang, Z.L. Chen, C. Wang, W.M. Cao, X. Zhang, Z.P. Ping, C.M. Liu, J.Y. Liu, Z.J. Li and J.C. Li. 2015. Serum protein S100A9, SOD3, and MMP9 as new diagnostic biomarkers for pulmonary tuberculosis by iTRAQ-coupled two-dimensional LC-MS/MS. *Proteomics,* 15: 58-67.

Xu, X.Y., R. Fan, R. Zheng, C.M. Li and D.Y. Yu. 2011. Proteomic analysis of seed germination under salt stress in soybeans. *J. Zhejiang Univ. Sci., B.,* 12: 507-517.

Zhang, L., Z.F. Yu, L. Jiang, J. Jiang, H.B. Luo and L.R. Fu. 2011. Effect of post-harvest heat treatment on proteome change of peach fruit during ripening. *J. Proteomics,* 74: 1135-1149.

Zhang, P.J., C.H. Li, P. Zhang, C.H. Jin, D.D. Pan and Y.B. Bao. 2014. iTRAQ-Based proteomics reveals novel members involved in pathogen challenge in sea cucumber *Apostichopus japonicus*. *Plos One,* 9: 1-9.

Zheng, M., Y.H. Wang, K. Liu, H.M. Shu and M.G. Zhou. 2012. Protein expression changes during cotton fiber elongation in response to low temperature stress. *J. Plant Physiol.,* 169: 399-409.

Zhao, Q., H. Zhang, T. Wang, S.X. Chen and S.J. Dai. 2013. Proteomics-based investigation of salt-responsive mechanisms in plant roots. *J. Proteomics.,* 82: 230-253.

Zhu, J.K. 2001. Plant salt tolerance. *Trends Plant Sci.,* 6: 66-71.

(Received for publication 16 July 2016)